



McpT, a Broad-Range Carboxylate Chemoreceptor in Sinorhizobium meliloti

Hiba Baaziz, a K. Karl Compton, a Sherry B. Hildreth, a Richard F. Helm, b Birgit E. Scharfa

^aDepartment of Biological Sciences, Virginia Tech, Blacksburg, Virginia, USA

ABSTRACT Chemoreceptors enable the legume symbiont Sinorhizobium meliloti to detect and respond to specific chemicals released from their host plant alfalfa, which allows the establishment of a nitrogen-fixing symbiosis. The periplasmic region (PR) of transmembrane chemoreceptors act as the sensory input module for chemotaxis systems via binding of specific ligands, either directly or indirectly. S. meliloti has six transmembrane and two cytosolic chemoreceptors. However, the function of only three of the transmembrane receptors have been characterized so far, with McpU, McpV, and McpX serving as general amino acid, short-chain carboxylate, and quaternary ammonium compound sensors, respectively. In the present study, we analyzed the S. meliloti chemoreceptor McpT. High-throughput differential scanning fluorimetry assays, using Biolog phenotype microarray plates, identified 15 potential ligands for McpTPR, with the majority classified as mono-, di-, and tricarboxylates. S. meliloti exhibited positive chemotaxis toward seven selected carboxylates, namely, α -ketobutyrate, citrate, glyoxylate, malate, malonate, oxalate, and succinate. These carboxylates were detected in seed exudates of the alfalfa host. Deletion of mcpT resulted in a significant decrease of chemotaxis to all carboxylates except for citrate. Isothermal titration calorimetry revealed that McpTPR bound preferentially to the monocarboxylate glyoxylate and with lower affinity to the dicarboxylates malate, malonate, and oxalate. However, no direct binding was detected for the remaining three carboxylates that elicited an McpT-dependent chemotaxis response. Taken together, these results demonstrate that McpT is a broad-range carboxylate chemoreceptor that mediates chemotactic response via direct ligand binding and an indirect mechanism that needs to be identified.

IMPORTANCE Nitrate pollution is one of the most widespread and challenging environmental problems that is mainly caused by the agricultural overapplication of nitrogen fertilizers. Biological nitrogen fixation by the endosymbiont *Sinorhizobium meliloti* enhances the growth of its host *Medicago sativa* (alfalfa), which also efficiently supplies the soil with nitrogen. Establishment of the *S. meliloti*-alfalfa symbiosis relies on the early exchange and recognition of chemical signals. The present study contributes to the disclosure of this complex molecular dialogue by investigating the underlying mechanisms of carboxylate sensing in *S. meliloti*. Understanding individual steps that govern the *S. meliloti*-alfalfa molecular cross talk helps in the development of efficient, commercial bacterial inoculants that promote the growth of alfalfa, which is the most cultivated forage legume in the world, and improves soil fertility.

KEYWORDS chemotaxis, legume, rhizobia, symbiosis

esponding to changes in environmental conditions is a fundamental strategy of bacteria to survive and proliferate (1, 2). Bacteria have evolved an advanced sensing mechanism, named chemotaxis, that allows them to rapidly respond to chemical

Citation Baaziz H, Compton KK, Hildreth SB, Helm RF, Scharf BE. 2021. McpT, a broad-range carboxylate chemoreceptor in *Sinorhizobium meliloti*. J Bacteriol 203:e00216-21. https://doi .orq/10.1128/JB.00216-21.

Editor Anke Becker, Philipps University Marburg

Copyright © 2021 American Society for Microbiology. All Rights Reserved.

Address correspondence to Birgit E. Scharf, bscharf@vt.edu.

Received 27 April 2021 Accepted 27 May 2021

Accepted manuscript posted online

14 June 2021

Published 9 August 2021

^bDepartment of Biochemistry, Virginia Tech, Blacksburg, Virginia, USA

gradients in their surroundings by approaching chemically favorable environments and avoiding hostile ones (3). Bacterial chemotaxis is implicated in the establishment of the symbiosis between Fabaceae (legumes) and nitrogen-fixing soil bacteria, referred to as rhizobia. Rhizobia sense signaling biomolecules released by germinating host seeds and developing roots and modulate their swimming direction toward increasing concentrations of these compounds accumulated in the spermosphere and rhizosphere (4).

Chemotaxis of the soil-dwelling alphaproteobacterium Sinorhizobium meliloti plays a key role in triggering colonization of the roots of its host legume Medicago sativa (alfalfa), ultimately resulting in the development of symbiotic root nodules populated by nitrogen-fixing S. meliloti bacteroids (5, 6). Prior to nodulation, germinating alfalfa seeds exude a large variety of signaling metabolites, including sugars, amino acids, organic acids, and quaternary ammonium compounds that act as chemoattractants for S. meliloti (4, 7-10). Typically, signal perception is mediated through the sensory domains of chemoreceptors, known as methyl-accepting chemotaxis proteins (MCPs). The direct binding of chemoattractants to the sensory domain called the ligand binding domain (LBD) is the most common mechanism of signal perception by MCPs (11). However, sensing can also be indirect through binding of the ligand to cognate periplasmic binding proteins (BPs). The ligand-BP complexes are then able to bind to the LBD and consequently trigger the chemotactic response (12). A well-studied example of indirect ligand sensing is maltose chemotaxis in Escherichia coli, where a periplasmic maltosebinding protein binds maltose prior to an interaction with the sensory domain of the chemoreceptor Tar (13, 14).

Some sensory domains can also bind cofactors, such as heme or flavin adenine dinucleotide (FAD), which allow chemoreceptors to detect oxygen and changes in redox status (15, 16). In the intensely studied E. coli signaling pathway, signal perception by the periplasmic LBDs of four transmembrane chemoreceptors (Tap, Tar, Trg, and Tsr) and the cytoplasmic sensory domain of Aer generates a molecular stimulus that modulates the autophosphorylation activity of the histidine autokinase CheA, which in turn alters transphosphorylation kinetics to the response regulator CheY. Phosphorylated CheY interacts with the flagellar motor to control the direction of flagellar rotation and to ultimately mediate chemotaxis (2, 16-20). In contrast, S. meliloti harbors genes coding for six transmembrane chemoreceptors (McpT, McpU, McpV, McpW, McpX, and McpZ) as well as two cytosolic receptors (McpY and IcpA). To modulate swimming behavior, chemoreceptor signaling domains convey sensory information to the flagellar motors, controlling the variation in its rotary speed via a complex signal transduction pathway that includes nine chemotaxis proteins (CheA, CheB, CheD, CheR, CheS, CheT, CheW, CheY1, and CheY2) (21).

Different structural organizations have been described for transmembrane chemoreceptors, and the most common one is typified by the E. coli receptors Tar and Tsr (18). These receptors consist of a variable periplasmic region (PR) flanked by two transmembrane helices, followed by a histidine kinase, adenyl cyclase, MCP, and phosphatase (HAMP) domain and a highly conserved cytoplasmic signaling domain (18, 22). We have shown previously that S. meliloti chemoreceptors McpU, McpV, and McpX, of which their PRs contain cache domains (calcium channels and chemotaxis receptors), sense plant-derived amino acids, short-chain carboxylates, and quaternary ammonium compounds, respectively, via direct binding (7-9, 21). The transmembrane chemoreceptor McpT (GenBank accession no. AF312875) is 652 amino acids (aa) long and consists of a periplasmic region of 150 aa, which harbors the ligand binding domain, two transmembrane domains, and a cytoplasmic region with two methylation helices, a signaling domain, and two HAMP domains (see Fig. S1 in the supplemental material) (21). The characterization of McpT function as well as its mode of attractant recognition is a focus of the present study. We show that McpT is a broad-range sensor for alfalfaderived carboxylates. We also demonstrate that McpTPR can recognize carboxylates through direct binding and additionally through a yet-to be identified indirect binding

mechanism. Overall, our study illustrates that alfalfa-exuded carboxylates play a role in the symbiotic signaling between S. meliloti and alfalfa because S. meliloti employs at least two chemoreceptors, namely, McpT and McpV, to ensure sensing of a wide range of host-borne carboxylates.

RESULTS

A high-throughput DSF assay identifies carboxylates as putative ligands of McpT. Bacteria have evolved chemotactic behavior for a vast variety of beneficial chemicals, such as carbon and nitrogen compounds, and energy sources secreted by their symbiotic host (1, 23). To test for potential interactions of these types of compounds with McpT, the periplasmic region of McpT (McpTPR; McpT₁₇₋₁₆₆) was recombinantly expressed and purified by affinity and size exclusion chromatography. A high-throughput in vitro differential scanning fluorimetry (DSF) assay using Biolog phenotype microarray (PM) plates as templates was then used to screen for potential ligands of McpTPR (24). Typically, the binding of a ligand stabilizes the protein causing an increase of its melting temperature (T_m) . The DSF assay using Biolog phenotype microarray plates helps rapid screening of ligand binding by measuring the difference in the protein temperature midpoint of unfolding (ΔT_m) in the presence and absence of potential ligands. We screened the recombinant McpTPR against the compounds present in Biolog phenotype microarray plates PM1 and PM2A, which represent 190 carbon sources (sugars, carboxylates, amino acids, and organic acids), as well as PM3B containing 95 nitrogen sources.

In the absence of ligands, McpT^{PR} displayed a T_m of 33 \pm 0.5°C. The melting temperature of the McpTPR in the presence of most compounds was within 1 to 2°C of the control; therefore, an interaction was defined as a T_m shift of >2.5°C. Of the 285 potential ligands screened, no positive interaction was observed with compounds from plate PM3B, and 15 compounds from PM1 and PM2A caused temperature shifts with ΔT_m values of >2.5°C (Fig. 1; see Fig. S2 in the supplemental material). Twelve of these compounds were identified as mono-, di-, and tricarboxylates. The monocarboxylates α -ketobutyrate and glyoxylate elicited the greatest thermal shifts with a ΔT_m of 5°C, followed by propionate that resulted in a ΔT_m of 4°C. The dicarboxylates L-malate, Dmalate, and D-, L-malate, as well as the monocarboxylate acetate, led to a ΔT_m of 3.5°C. The T_m of McpTPR shifted by 3°C in the presence of the dicarboxylates malonate, tartrate, and oxalate, and the tricarboxylate oxalomalate. The lowest shift close to background level (ΔT_m of 2.5°C) was elicited by the dicarboxylate succinate and the tricarboxylate citrate (Fig. 1). In addition to carboxylates, three carboxylate derivatives, namely, methyl-p-lactate, citramalate, and salicylate, exhibited ΔT_m values above the threshold of 2.5°C (Fig. 1).

Although DSF screening using Biolog phenotype microarray plates provides rapid information on putative ligands, it does not represent definitive proof of binding, as proteins can interact with the minimal medium present in the Biolog phenotype microarray plate wells causing false-positive results. Therefore, binding of the 12 carboxylates identified as potential ligands of McpTPR was tested with defined ligand solutions. The DSF assay was performed at three different ligand concentrations (0.4, 4, and 40 mM) to test whether the protein T_m increases with fractional ligand occupancy (25). Acetate, propionate, and tartrate at 40 mM resulted in ΔT_m shifts lower than the threshold of 2.5°C. In addition, increasing concentrations of these three compounds did not increase the thermal stability of the protein (Fig. S2). Taken together, the results tentatively indicate that acetate, propionate, and tartrate might not be ligands for McpTPR. However, increasing concentrations of the remaining carboxylates resulted in a statistically significant increase in the thermal stability of the protein, confirming that they are potential ligands for McpTPR (Fig. 2). It is noteworthy that the greatest thermal shift of 11°C was elicited by malonate at a concentration of 40 mM. Glyoxylate and oxalomalate followed with a ΔT_m of 6.75°C and 6.5°C, respectively, at 40 mM (Fig. S2).

S. meliloti wild type is attracted to carboxylates. The chemotactic response of S. meliloti wild type (RU11/001) toward seven representative potential ligands of McpT, namely, α -ketobutyrate, citrate, glyoxylate, L-malate, malonate, oxalate, and succinate,

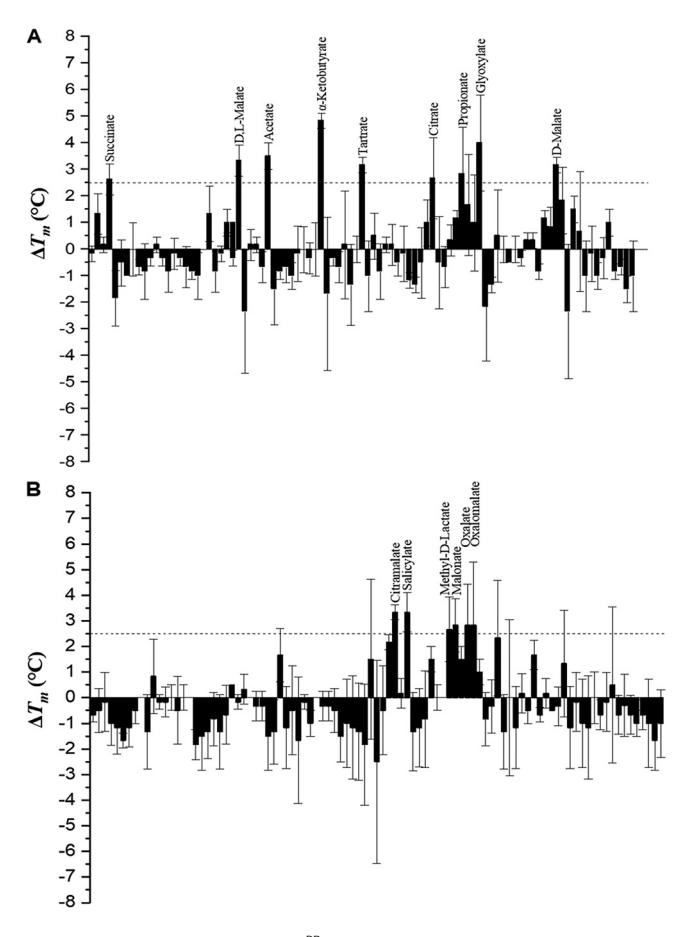


FIG 1 High-throughput DSF screen of McpT^{PR} with 190 potential ligands from Biolog phenotype microarray plates PM1 (A) and PM2B (B). The $\Delta T_{\rm m}$ is the change in thermal stability of recombinant $\mathrm{McpT^{PR}}$ in the presence of a compound. ΔT_{m} values above the threshold (dotted line) of 2.5°C indicate a possible ligand-protein interaction. The compounds identified as potential McpT ligands are labeled. Values are the means and standard deviations from three biological replicates.

was tested with quantitative capillary assays. In these assays, the response is quantified by comparing the numbers of cells that navigate into a capillary containing a potential chemoattractant to the number of cells that accumulate in a capillary containing only Rhizobium basal (RB) medium. The chemotactic response was measured over a range of concentrations for each ligand (10 μ M to up to 2 M). The S. meliloti wild type showed positive chemotaxis toward all seven carboxylates (Fig. 3). The compounds elicited a concentration-dependent chemoattraction curve that peaked and subsequently decreased, except for malonate, succinate, and oxalate where the curve peaked at their solubility limit in RB medium. The wild-type strain was attracted to α -ketobutyrate, glyoxylate, oxalate, and succinate with a chemoattraction peak at 10, 100, 250, and 400 mM, respectively. Malate elicited a large chemoattraction plateau between 100 mM and 1 M, while the attraction to malonate peaked at 2 M. In contrast, chemoattraction to citrate was observed only at lower concentrations and peaked at $100\,\mu\text{M}$. At peak concentration, oxalate and glyoxylate caused the greatest accumulation with 61,000 and 52,000 cells per capillary. Succinate, malonate, and malate followed each with 35,000, 31,500 and 30,000 cells per capillary, respectively. The peak concentration of α -ketobutyrate elicited an accumulation of 23,300 cells per capillary. Citrate displayed the lowest accumulation with only 14,000 cells per capillary (Fig. 3). To demonstrate that the observed S. meliloti attraction toward high concentrations of carboxylates is not due to any osmotic effects, the chemotactic response of S. meliloti wild type toward a range of NaCl concentrations (10 mM to 4 M) was investigated. No

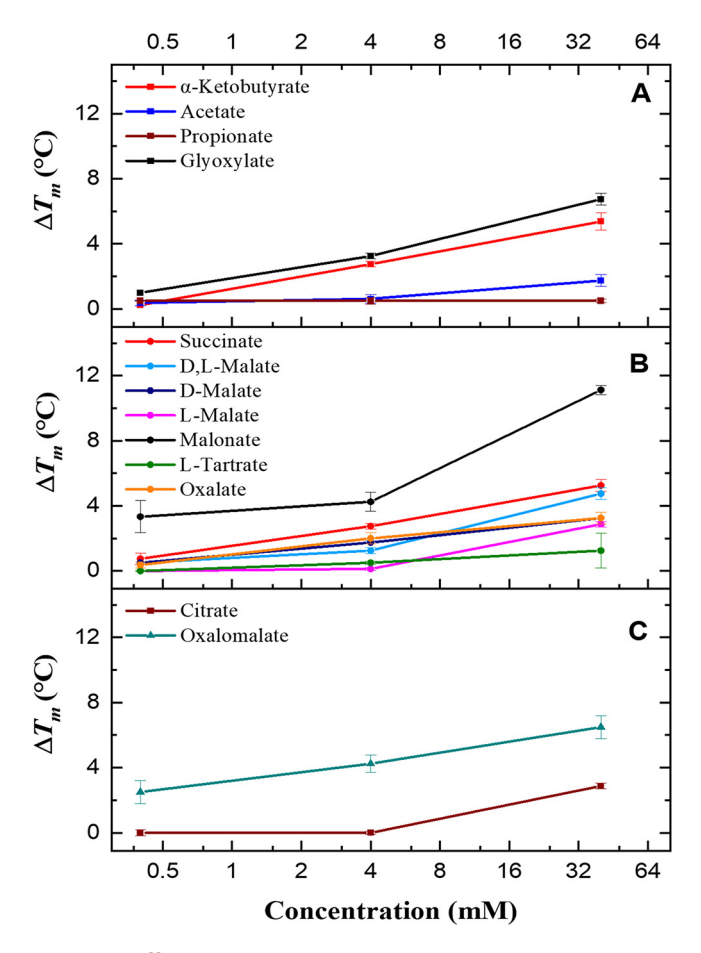


FIG 2 DSF screen of McpTPR with various concentrations of potential ligands. (A) Monocarboxylates; (B) dicarboxylates; (C) tricarboxylates. Specifically, compounds were tested at concentrations of 0.4, 4.0, and 40 mM. Data are the means and standard deviations from three biological replicates. If not visible, the error bars are contained within the symbol.

attraction was detected toward any of the tested NaCl concentrations (see Fig. S3 in the supplemental material).

McpT mediates carboxylate sensing in S. meliloti. To investigate the impact of McpT on carboxylate sensing, the chemotaxis response of a strain lacking mcpT (RU11/ 838) was tested toward different concentrations of the seven selected carboxylates. In the absence of mcpT, S. meliloti chemotaxis to carboxylates was significantly decreased (Fig. 4). For succinate, the number of $\Delta mcpT$ cells accumulated at the peak concentration (400 mM) was 6-fold lower than that of the wild type. Moreover, chemoattraction of the $\Delta mcpT$ strain to the peak concentrations of malate (1 M), malonate (2 M), and oxalate (250 mM) was decreased by 4-fold, while attraction to the peak concentration of α -ketobutyrate (10 mM) and glyoxylate (100 mM) was 3-fold lower. It is noteworthy that in the absence of mcpT, the peak response of α -ketobutyrate was shifted to a higher concentration (100 mM), which indicates that cells became less sensitive (Fig. 4 and 5). Finally, chemotaxis of the mcpT deletion strain toward citrate was only marginally reduced by 1.5-fold at peak concentration (0.1 mM) (Fig. 4 and 5).

Since McpV is also a sensor of carboxylates, we performed chemotaxis assays with BS275, a strain lacking mcpT and mcpV. The double-deletion strain displayed a severe, 13-fold decrease of chemotaxis to the peak concentration of oxalate. Furthermore, the absence of both MCPs abolished α -ketobutyrate, citrate, and glyoxylate sensing (Fig. 5). These results indicate that both McpT and McpV might be involved in the recognition of α -ketobutyrate, citrate, glyoxylate, and oxalate. However, the chemoattraction

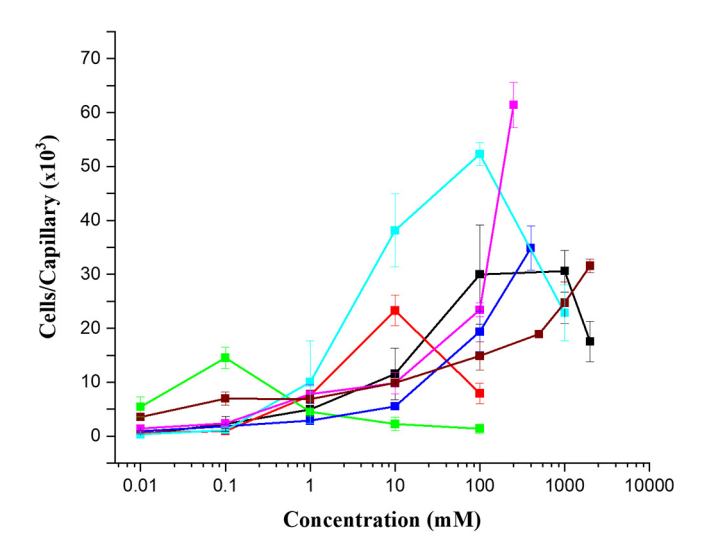


FIG 3 Chemotaxis responses of S. meliloti wild type toward carboxylates in a quantitative capillary assay. Response curves to α -ketobutyrate (red), citrate (green), glyoxylate (light blue), malate (black), malonate (brown), oxalate (purple), and succinate (dark blue). Data have been normalized to a negative control by subtracting the average number of cells that accumulated in control capillaries containing only RB medium. The data represent the mean and standard deviation from at least four independent biological replicates.

of the double-deletion strain to the peak concentration of malate, malonate, and succinate was similar to that of the mcpT-deletion strain, demonstrating that McpV is not implicated in the sensing of these carboxylates (Fig. 5). It should be noted that the absence of either McpT or McpT and McpV did not negatively impact the chemotaxis ability toward other attractants, as strains $\Delta mcpT$ and $\Delta mcpT$ $\Delta mcpV$ reacted to proline, which is sensed by McpU and McpX, with the same strength as the wild-type strain (see Fig. S4 in the supplemental material). Moreover, the introduction of the complementing plasmid pBBR1MCS-2 constitutively expressing mcpT (pBS1056) to the ∆mcpT strain (RU11/838) restored chemotaxis toward carboxylates to wild-type levels (Fig. 5).

To fully attribute the observed bacterial accumulation in the capillaries to a chemotaxis response, attraction of a strain lacking all chemoreceptors (Che-; strain RU13/ 149) toward the seven carboxylates was tested. Chemotaxis to α -ketobutyrate, citrate, glyoxylate, succinate, and oxalate was indeed severely diminished (Fig. 5). Surprisingly, chemotaxis toward the peak concentration of malate and malonate was observed at levels similar to those of the $\Delta mcpT$ strain (5,000 and 6,900 cells per capillary, respectively). To investigate whether the observed residual attraction is a true chemotaxis response, the reaction of wild type and the $\Delta mcpT$, $\Delta mcpT$ $\Delta mcpV$, and $\Delta che1$ strains toward malonate was analyzed in the absence of a concentration gradient by adding 100 mM malonate to both the bacterial ponds and the capillaries. None of S. meliloti strains tested showed an attraction toward malonate, confirming that the weak reaction of the Che-strain appears to be a chemotaxis response (Fig. 6).

Isothermal titration calorimetry demonstrates direct binding of specific carboxylates to McpTPR. To quantitatively assess the direct binding of chemoattractants to McpTPR, we used isothermal titration calorimetry (ITC). Initial titrations with α -ketobutyrate, citrate, malate, succinate, and glyoxylate at 10°C did not result in binding (Table 1). However, oxalate interacted with McpTPR, and the equilibrium dissociation constant (K_D) was measured at 248 nM, with an enthalpy change of -7,533 cal/ mol, an entropy change of 3.62 cal/mol/K, and an apparent binding stoichiometry of 0.21 (Fig. 7A; Table 1). When titrating McpTPR against malonate, we observed an initial exothermic peak followed by several endothermic peaks (see Fig. S5 in the supplemental material). This finding suggests that more than one interaction occurred, thus prohibiting the quantification of the McpTPR-malonate interaction. We have observed this

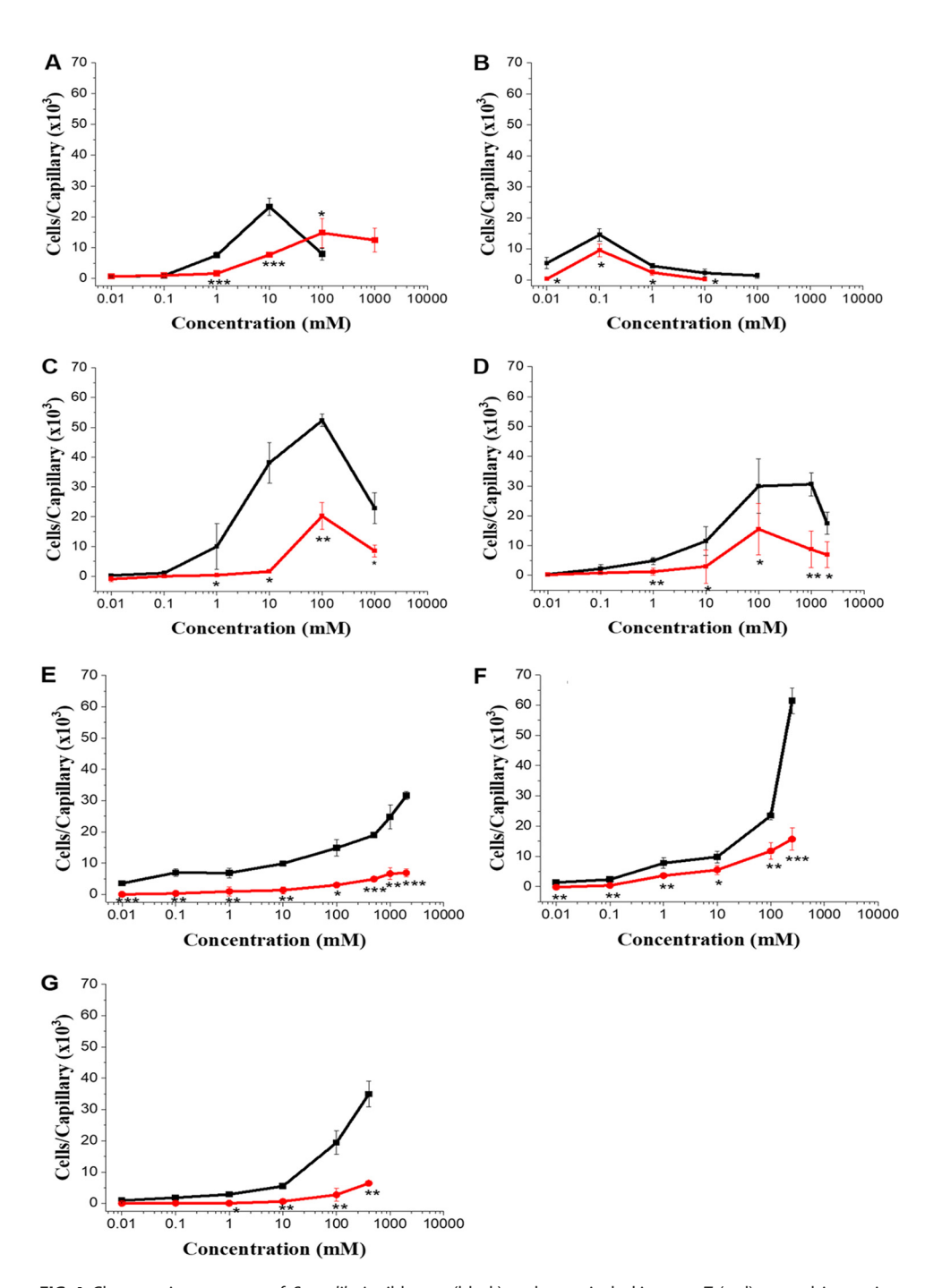


FIG 4 Chemotaxis responses of S. meliloti wild type (black) and a strain lacking mcpT (red) toward increasing concentrations of potential ligands. (A) α -Ketobutyrate; (B) citrate; (C) glyoxylate; (D) malate; (E) malonate; (F) oxalate; (G) succinate. Chemotaxis data of the wild-type response are taken from Fig. 3. Values are the means and standard deviations from at least four biological replicates. If not visible, the error bars are contained within the symbol. Asterisks denote P values determined by Student's t test; *, P < 0.05; **, P < 0.01; ***, P < 0.01;

type of ambiguous interaction in previous chemoreceptor studies (8). Some binding interactions do not create observable heat signals when the changes in enthalpy and entropy are equal and opposite, but this can be overcome by repeating experiments at a different temperature (26). We repeated experiments at 10°C but found that α -ketobutyrate and citrate still did not exhibit binding. In contrast, succinate, malate, and glyoxylate bound to McpT^{PR} at 20°C, with a K_D of 680 μ M, 813 μ M, and 284 μ M,

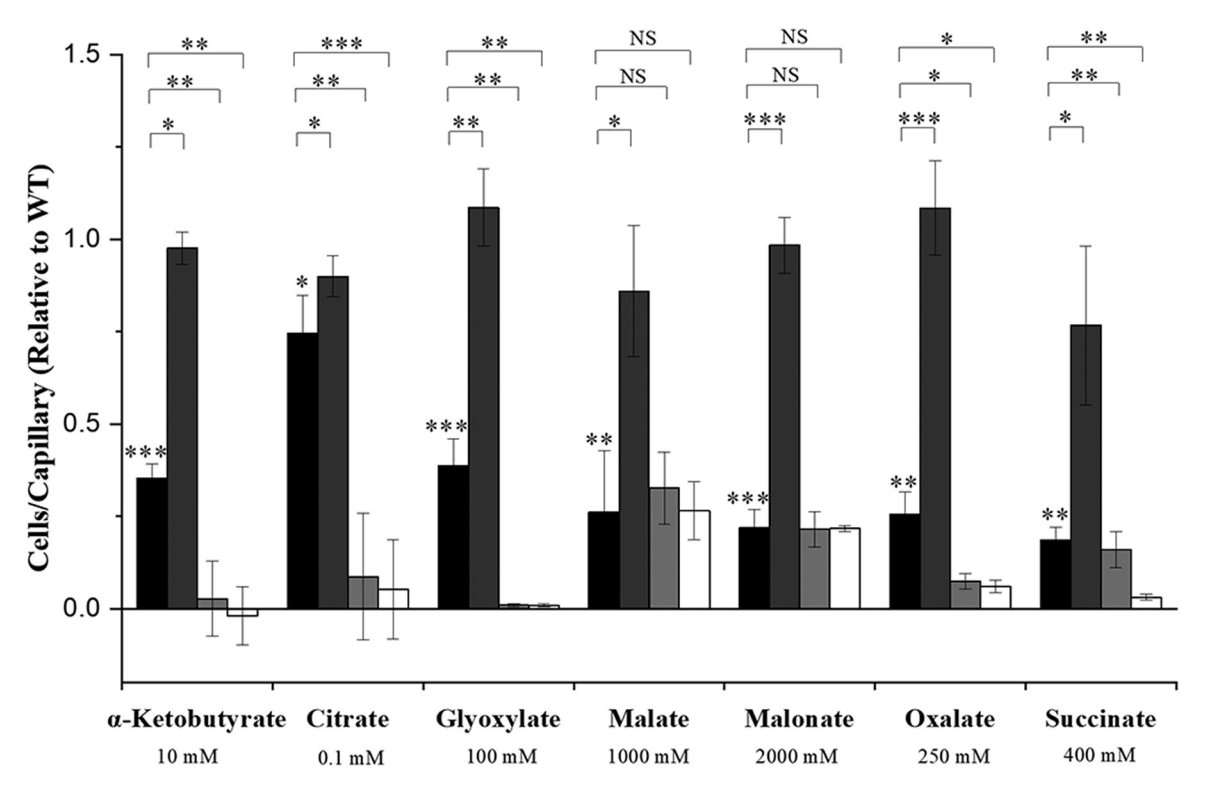


FIG 5 Chemotactic responses of various S. meliloti deletion strains to selected carboxylates relative to wild type. Black bars, ΔmcpT (RU11/838); dark gray bars, $\Delta mcpT/mcpT$ (RU11/838 with pBS1056); light gray bars, $\Delta mcpT$ $\Delta mcpV$ (BS275); white bars, Che- (RU13/808); dark gray bars, $\Delta mcpT$ $\Delta mcpV$ (BS275); white bars, Che- (RU13/808); light gray bars, $\Delta mcpT$ $\Delta mcpV$ (BS275); white bars, Che- (RU13/808); light gray bars, $\Delta mcpT$ $\Delta mcpV$ (BS275); white bars, Che- (RU13/808); light gray bars, $\Delta mcpT$ $\Delta mcpV$ (BS275); white bars, Che- (RU13/808); light gray bars, $\Delta mcpT$ $\Delta mcpV$ (BS275); white bars, Che- (RU13/808); light gray bars, $\Delta mcpT$ (RU11/808); light gray bars, Δm 149). The average number of cells per capillary for each strain was normalized to that of wild type. Values are the means and standard deviations from at least four biological replicates. Asterisks denotes P values determined by Student's t test; *, P < 0.05; **, P < 0.01; ***, P < 0.0001; NS, not significant (P > 0.05). P values above $\Delta mcpT$ represent significant differences compared with wild type.

respectively. A hyperbolic isotherm was achieved with 15 μ M protein in the titration with malonate at 20°C, yielding a K_D of 4.0 μ M. In addition, the affinity of McpT^{PR} for oxalate was reduced at the higher temperature, yielding a K_D of 2.0 μ M (Fig. 7B; Table 1). It should be noted that all binding reactions with McpTPR at 20°C were exothermic. Taken together, these data indicate that McpT directly binds specific carboxylates to control sensing of the respective attractants.

Analytical size exclusion chromatography and isothermal titration calorimetry suggest the formation of McpTPR dimers. A structure-based homology search using the Swiss-Model repository predicted that the McpT periplasmic region classifies as a four-helix bundle (Fig. S1). This type of fold is an obligate dimer. To support this prediction, we performed analytical size exclusion chromatography with McpTPR and compared its retention time (RT) to that of molecular weight (MW) standards. McpTPR eluted in a single peak at an RT of 15.8 ml, after ovalbumin (RT, 15.4 ml), which has a MW of 44 kDa. Monomeric McpTPR has a molecular weight of 18.3 kDa, suggesting that the McpTPR population exists entirely as a dimer (36.6 kDa) (Fig. 8). Amending the chromatography buffer with any of the ligands tested in the ITC analysis did not significantly alter the retention time of the protein (data not shown).

To further characterize the dimerization of McpT, we used isothermal titration calorimetry to determine the dimer dissociation constant. We hypothesized that if McpTPR exists in solution as a dimer, it would dissociate when diluted during injections into the buffer and generate a thermal signal. Injections of McpTPR into buffer yielded a hyperbolic endothermic reaction, and the K_D was determined to be 1.3 μ M (Fig. 9A). We repeated this experiment with ligand added to the protein and the buffer solution in the cell. With the addition of 10 mM malate, 1.1 mM glyoxylate, and 10 mM succinate, the K_D of the McpT^{PR} dimer was between 0.8 and 2.1 μ M (Fig. 9B). In the presence

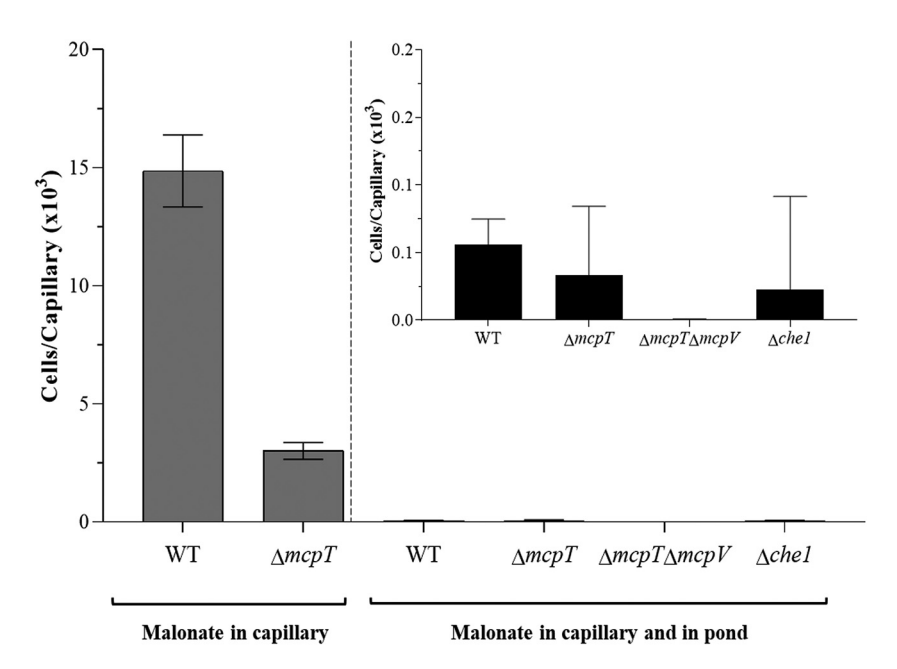


FIG 6 Chemotactic responses of various *S. meliloti* strains to malonate in the absence of a concentration gradient. Attraction toward 100 mM malonate in capillaries was tested in bacterial ponds with 100 mM malonate (main graph and inset). Chemotaxis data of the wild-type and $\Delta mcpT$ (RU11/838) response in the presence of a concentration gradient with 100 mM malonate in capillaries but not in bacterial ponds (gray bars) were taken from Fig. 4. Note the difference in scale between the main graph and inset. Values are the means and standard deviations from three biological replicates.

of 0.1 mM oxalate, no signal was observed, indicating that dissociation of McpT^{PR} dimers did not occur (Fig. 9A). Together, these results demonstrate the propensity of McpT^{PR} to dimerize and support our model that it adopts a four-helix bundle domain.

Carboxylates are present in alfalfa seed exudates. Since behavioral experiments showed that *S. meliloti* is attracted to α -ketobutyrate, citrate, glyoxylate, malate, malonate, oxalate, and succinate, we investigated the presence of these carboxylates in germinating alfalfa seed exudates using liquid chromatography-mass spectrometry (LC-MS). The data analysis revealed that all compounds but α -ketobutyrate were exuded in amounts above the quantification limit (0.14 nmol/seed) and ranged from 0.5 to 10 nmol per seed. With an average seed volume of 2.17 μ l, the concentration of glyoxylate, malate, malonate, citrate, and oxalate at the surface of the seed was calculated to range from 4.64 mM to 0.2 mM with an approximate ratio of 10:1:0.5 for malate/citrate, malonate/oxalate, and glyoxylate/succinate, respectively. These results show that carboxylates are secreted by germinating alfalfa seeds at millimolar concentrations, which are able to elicit a chemotactic response in *S. meliloti* (Fig. 4 and Table 2).

DISCUSSION

Given the massive microbial diversity in the soil, the possibility that a plant recruits a specific bacterial symbiont by chance is very low. To attract the soil-dwelling *S. meliloti*, alfalfa exudes specific signaling molecules into the spermo- and rhizosphere, such as primary metabolites like amino acids and organic acids (4, 7–10). Chemotaxis enables bacterial cells to locate host plant roots and germinating seeds by sensing their exudates (5, 6). This process is mediated by arrays of chemoreceptors (MCPs). In the present study, we report the contribution of the *S. meliloti* chemoreceptor McpT to chemotaxis toward a broad spectrum of carboxylates.

We first elucidated the ligand profile of McpT with a high-throughput *in vitro* screen. McpT^{PR} appeared to interact with a range of mono-, di-, and tricarboxylates, indicating that McpT might interact with negatively charged organic compounds (Fig. 1). This

TABLE 1 Affinity of McpT^{PR} for carboxylates

	K_D by compound ^a								
Temp (°C)	α -Ketobutyrate	Citrate	Glyoxylate	Malate	Malonate	Oxalate	Succinate		
10 ^b	N/B	N/B	N/B	N/B	N/D	248 nM	N/B		
20 ^c	N/B	N/B	$284\mu{ m M}$	$813\mu\mathrm{M}$	$4.0\mu\mathrm{M}$	$2.0\mu\mathrm{M}$	$680\mu\mathrm{M}$		

^aN/B, no binding; N/D, not determined.

finding compelled us to conduct quantitative behavioral capillary experiments to determine the physiological response to these carboxylates. S. meliloti exhibited a variable magnitude of chemotactic responses to the tested carboxylates. Glyoxylate, malate, malonate, oxalate, succinate, and oxalate elicited higher magnitudes of response than α -ketobutyrate and citrate (Fig. 3). Deletion of mcpT caused a significant reduction in chemotaxis toward all carboxylates, which indicates the implication of McpT in carboxylate sensing (Fig. 4 and 5).

We found that the absence of mcpT and mcpV abolished chemotaxis to α -ketobutyrate, citrate, and glyoxylate and severely reduced sensing of oxalate (Fig. 5), illustrating that McpT and McpV are both involved in carboxylate chemotaxis. An overlapping ligand spectrum has been reported for Pseudomonas aeruginosa PAO1, which relies on three chemoreceptors, namely, PctA, PctB, and PctC, to sense amino acids (24, 27, 28). Interestingly, in strains lacking either mcpT and mcpV, all MCPs still exhibited a weak response toward malate and malonate that was comparable to that of the mcpT strain (Fig. 5). This response can be attributed to chemotaxis because the attraction of these strains toward malonate was abolished in the absence of the concentration gradient (Fig. 6). We can only speculate whether this behavior is attributable to a regulation of flagellar motility via the second messenger 3',5'-cyclic di-GMP resulting from malate and malonate metabolism (29), although further studies are required to confirm this speculation.

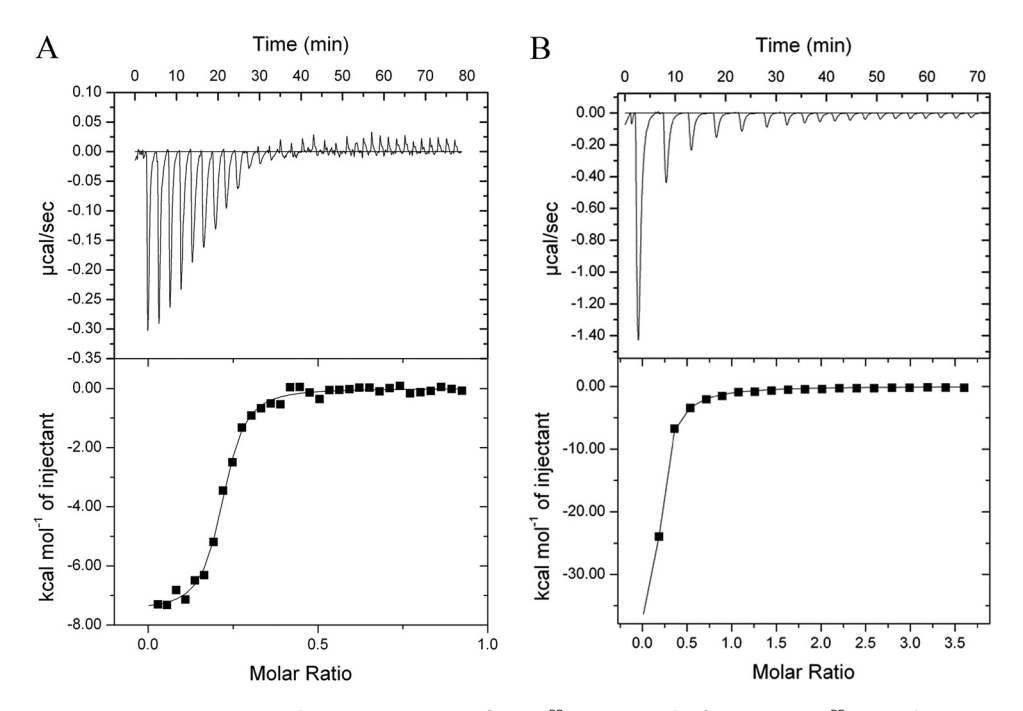


FIG 7 Representative microcalorimetry titrations of McpT^{PR}. (A) A total of $45\,\mu\text{M}$ McpT^{PR} titrated against 250 μM oxalate at 10°C; (B) 15 μM McpT^{PR} titrated against 1 mM malonate at 20°C. The curves of best fit were created using the "one binding site" function in the MicroCal version of Origin 7.

^bExperiments at 10°C were performed with 45 μ M McpT^{PR}.

Experiments at 20°C were performed with 45 μ M McpTPR, except for the titration with oxalate and glyoxylate, which was performed with 15 μ M McpT^{PR}. Titrations with malonate generated biphasic curves that could not be fit to a one-binding site model. See Fig. S5.

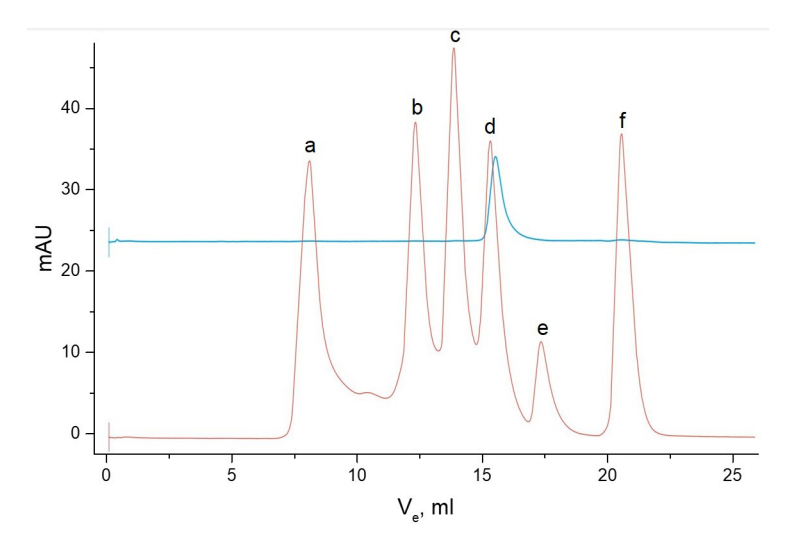


FIG 8 Analytical size exclusion chromatography of McpTPR (blue) compared with molecular weight standards (orange) in 0.1 M PIPES and 0.1 M KCl (pH 7.0). Samples were applied to the column in 200- μ l injections. a, dextran blue, 2,000 kDa; b, aldolase, 158 kDa; c, conalbumin, 75 kDa; d, ovalbumin, 44 kDa; e, cytochrome c, 12.4 kDa; f, vitamin B₁₂, 1.4 kDa.

Most of the characterized carboxylate sensors, such as McpV of S. meliloti and McpP of Pseudomonas putida KT2440, harbor cache signaling domains (8, 30). In contrast, homology modeling using Comamonas testosteroni MCP2201 and the asparate receptor of Salmonella enterica serovar Typhimurium (5xua.3.A and 2lig.1.B, respectively) suggests that McpTPR contains a 4-helix bundle domain fold, similar to the periplasmic domains of E. coli Tar and Tsr (31) (see Fig. S1 in the supplemental material). This type of domain typically forms obligate dimers, a prediction that is supported by analytical size exclusion chromatography of McpTPR (Fig. 8). Protein titrations of McpTPR into buffer also provided evidence for McpT homodimerization with a K_D of 1.3 μ M (Fig. 9A). When the titrations were performed with ligands in solution, the K_D did not change significantly. Therefore, no stabilizing effect was conferred by malate, glyoxylate, or succinate (Fig. 9B). The presence of 0.1 mM oxalate, however, obviated the dissociation signal, suggesting that the affinity between McpTPR monomers became too high to be detected with ITC (Fig. 9A). This behavior mirrors that of the aspartate receptor Tar, where ligand binding facilitates receptor dimerization (32). For McpTPR, it is possible that this effect occurred only in the presence of oxalate because of enhanced levels of receptor-ligand saturation.

To decipher the underlying molecular mechanism of carboxylate sensing by McpT, protein-ligand interactions were characterized using ITC. Surprisingly, only glyoxylate, malate, malonate, succinate, and oxalate were found to interact with McpTPR (Fig. 7; Table 1). Therefore, taxis to these five carboxylates is explained by the canonical direct binding described for many MCPs (23). In contrast, no binding to α -ketobutyrate or citrate was observed in ITC, although behavioral assays showed that McpT is responsible for the sensing of these carboxylates (Fig. 5 and S2). The most common explanation for this phenomenon is the mode of indirect binding, as described for E. coli taxis to maltose and the chemotaxis response of P. aeruginosa to low inorganic phosphate mediated through the interaction of the periplasmic binding protein PstS and the chemoreceptor CtpL (12, 14, 33). McpTPR had the highest affinity for oxalate and malonate, followed by glyoxylate, succinate, and then malate (Table 1). The primary determinant of the McpT ligand profile therefore appears to be size, as smaller ligands with 2 to 3 carbons are preferred. Charge is also important but appears to be a secondary factor because glyoxylate, with a charge of -1 and containing 2 carbons, had a greater affinity than malate and succinate, with each having a -2 charge and a 4-carbon chain

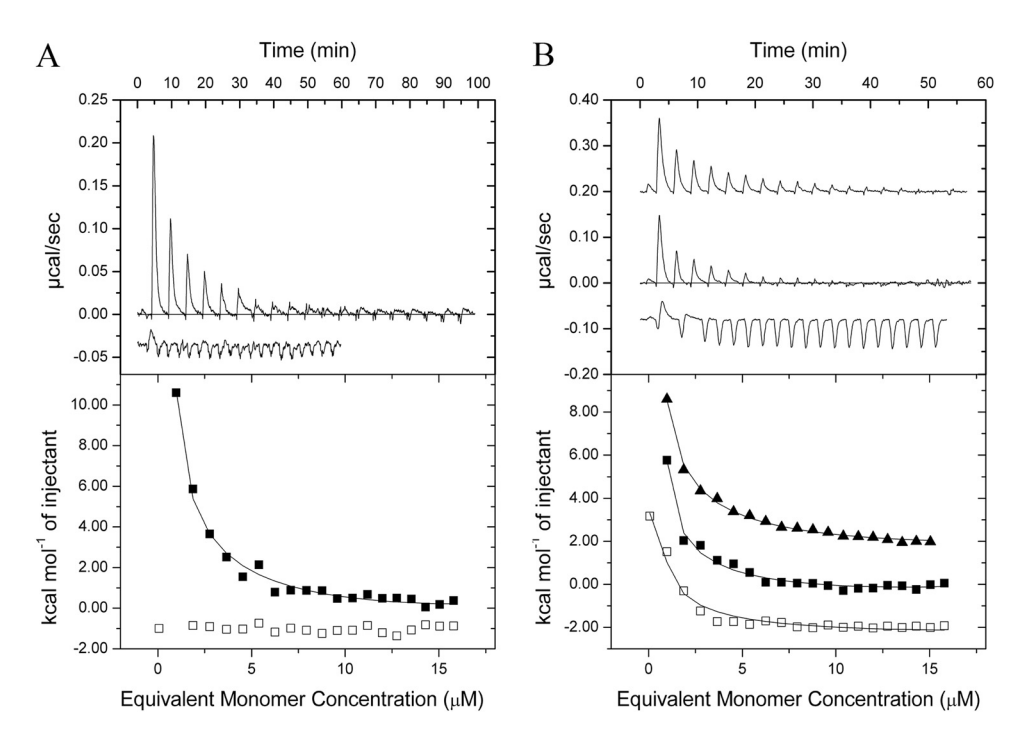


FIG 9 Titrations of McpT^{PR} into buffer or ligand solutions. (A) McpT^{PR} at a concentration of $90 \,\mu\text{M}$ was injected from the syringe into the cell containing buffer (top curve and filled boxes) or buffer with 0.1 mM oxalate (bottom curve and open boxes). (B) Titration of McpTPR into buffer containing 10 mM succinate (top curve, triangles), 10 mM malate (middle curve and filled boxes), or 1.1 mM glyoxylate (bottom curve and open boxes). For titrations into ligand solutions, the protein solution included the same concentration of the respective ligand. The curve of best fit was modeled to the thermogram using the "dissociation" model in the MicroCal version of Origin 7.

length. It is worth noting that ligands recognized by McpTPR through direct binding elicited stronger chemotactic responses than those potentially recognized indirectly.

To attribute the relevance of S. meliloti's carboxylate sensing to a host interaction, we investigated the presence of these attractants in alfalfa seed exudates. Our findings demonstrate that all seven carboxylate attractants of S. meliloti are exuded by germinating seeds of alfalfa (Table 2). Plant-derived carboxylates are known to play an important role in various biological processes in the rhizosphere, including mobilization and acquisition of essential nutrients (34). Malonate, oxalate, and succinate exuded by alfalfa release bioavailable manganese from manganese oxides through a combination of reduction and complexation processes (35). Exudation of citrate, glyoxylate, malate, and oxalate into the rhizosphere is an efficient mechanism for plants to increase phosphate solubility, which subsequently improves its acquisition (36–38). Rhizobia such as S. meliloti can utilize most plant-born carboxylates as carbon energy sources via the tricarboxylic acid (TCA) cycle, which explains their chemotactic responses toward these

TABLE 2 Amounts of carboxylates exuded by germinating alfalfa seeds

Compound	ng/seed ^a	nmol/seed	Concn on seed surface (mM)
α -Ketobutyrate	$<$ QL b	<ql< td=""><td><ql< td=""></ql<></td></ql<>	<ql< td=""></ql<>
Citrate	$1,829 \pm 418$	9.52 ± 2.17	4.39 ± 1.00
Glyoxylate	26 ± 3	0.35 ± 0.04	0.16 ± 0.02
Malate	$1,350 \pm 611$	10.07 ± 4.55	4.64 ± 2.10
Malonate	130 ± 39	1.25 ± 0.37	0.57 ± 0.17
Oxalate	97 ± 23	0.76 ± 0.18	0.35 ± 0.08
Succinate	57 ± 15	0.48 ± 0.13	0.22 ± 0.06

^aAll compounds were measured in nanograms per microliter of exudate and converted to nanograms per seed or nanomoles per seed based on the number of seeds in 0.1 g. Each value is the mean from five experiments and standard deviation of the mean.

b<OL, below quantification limit (0.14 nmol/seed).

TABLE 3 Bacterial strains and plasmids

Strain or plasmid	Characteristic(s) ^a	Reference or source
Strains		
E. coli		
DH5 α	recA1 endA1	51
ER2566	lon ompT lacZ::T7	New England BioLabs
S17-1	recA endA thi hsdR RP4-2 Tc::Mu::Tn7 Tp ^r Sm ^r	52
S. meliloti		
BS251	Sm ^r ; ∆ <i>che1</i> operon	This work
BS275	$Sm^r\Delta m cpT\Delta m cpV$	This work
RU11/001	Sm ^r ; spontaneous streptomycin-resistant wild-type strain	53
RU11/838	$Sm^r\Delta m c p T$	21
RU13/149	Sm $^{\text{r}}$ Δ mcp S Δ mcp T Δ mcp U Δ mcp V Δ mcp W Δ mcp Y Δ mcp Y Δ mcp Z Δ icp A (Δ 9)	21
Plasmids		
pBBR1MCS-2	Km ^r ; expression vector	54
pBS425	Apr; Sapl/Spel PCR fragment containing mcpT bp 48–498 (McpTPR, aa 17–166) cloned into pTYB11	This work
pBS1056	Km ^r ; HindIII/Xbal PCR fragment containing mcpT cloned into pBBR1MCS-2	This work
pTYB11	Ap ^r ; expression vector	New England BioLabs

aNomenclature is presented according to Bachmann (55) and Novick et al. (56). Tp/, trimethoprim resistance; Ap/, ampicillin resistance; Sm/, streptomycin resistance; Km/, kanamycin resistance.

compounds (39-43). The presence of carboxylates in alfalfa seed exudates together with the ability of S. meliloti to sense them highlight the importance of carboxylates in host-symbiont signaling. The use of carboxylates as signaling molecules to establish a symbiosis with soil bacteria has also been reported for the leguminous tree Sesbania rostrata and its rhizbobial symbiont Azorhizobium caulinodans ORS571 (44). Thus, having sensors spurring navigation to carbon sources and host signals such as carboxylates is clearly advantageous for soil bacteria.

Combining the documentation of physiological responses together with in vitro binding parameters grants a complete picture of how bacteria achieve taxis to chemoattractants. The present study expands our knowledge of S. meliloti's sensory repertoire by demonstrating that in addition to the previously identified short-chain monocarboxylate sensor McpV (8), S. meliloti employs McpT to sense a broader spectrum of carboxylates exuded by alfalfa, either via direct or a yet-to-be-identified indirect binding mechanism.

MATERIALS AND METHODS

Strains and plasmids. Derivative Escherichia coli K-12 strains, the highly motile derivatives of S. meliloti MV II-1 (45), and the plasmids used are listed in Table 3.

Media and growth conditions. Lysogeny broth (LB) was used to grow E. coli strains at 37°C (46). Tryptone-yeast extract-calcium chloride (TYC) medium supplemented with streptomycin (600 µg/ml) was used to grow S. meliloti strains at 30°C (47). Rhizobium basal (RB) medium [6.1 mM K,HPO_a, 3.9 mM ${\rm KH_2PO_{4^\prime}}\ 1\ {\rm mM\ MgSO_{4^\prime}}\ 1\ {\rm mM\ (NH_4)_2SO_{4^\prime}}\ 0.1\ {\rm mM\ CaCl_{2^\prime}}\ 0.1\ {\rm mM\ NaCl,\ 0.01\ mM\ Na_2MoO_{4^\prime}}\ 0.001\ {\rm mM\ FeSO_{4^\prime}}$ $20 \,\mu g$ of biotin/liter, and $100 \,\mu g$ of thiamine/liter] (48) layered on Bromfield agar plates at 30° C was used to grow motile cells of S. meliloti strains for capillary assays (49). Ampicillin and kanamycin were used for E. coli at the final concentrations of $100 \,\mu g/ml$ and $25 \,\mu g/ml$, respectively. For S. meliloti, neomycin and streptomycin were at the final concentrations of 120 μ g/ml and 600 μ g/ml, respectively.

Capillary assays. Traditional Adler capillary assays (50) with the modification described previously by Webb et al. (7) were performed. Briefly, S. meliloti cells were grown in RB medium overlain onto Bromfield agar plates for 16 h at 30°C. Cells were gently harvested between an optical density at 600 nm $({\rm OD_{600}})$ of 0.15 and 0.17 before being suspended in RB medium to a final ${\rm OD_{600}}$ of 0.15. To investigate the chemotaxis behavior in the absence of a malonate concentration gradient, cells were suspended in RB medium supplemented with 100 mM malonate. A total of 350 μ l of motile *S. meliloti* cells was injected into a pond formed from a U-shaped glass tube between two glass plates. Microcap glass 1-ul capillaries (Drummond Microcaps) flame sealed at one end were placed into various dilutions of the compound solution in a vacuum chamber to fill capillaries. Capillaries were placed into the bacterial ponds and left to incubate at room temperature for 2 hours. After incubation, the contents of the capillaries were expelled into 1-ml RB medium. Serial dilutions were plated on TYC plates supplemented with streptomycin, and subsequent counting of CFU was performed. The counts of control capillaries, containing only RB medium, were subtracted from all test capillaries. The accumulation of bacterial cells in the capillaries was calculated as the average from the CFU obtained in triplicate plates, and the results were expressed as the mean from at least four separate capillary assays for each compound and

concentration. The relative chemotaxis response was calculated as the ratio of the accumulation of the deletion mutant in the capillaries to that of the wild type.

Expression and purification of McpTPR. The recombinant ligand-binding, periplasmic region of McpT (McpT^{PR}; McpT₁₇₋₁₆₆) was overproduced from plasmid pTYB11 in *E. coli* ER2566, providing an intein-chitin-binding domain (intein-CBD) tag (Table 3). Four liters of cell culture was grown to an OD₆₀₀ of 0.8 at 37°C in LB containing 100 μg of ampicillin/ml, and gene expression was induced by 0.6 mM isopropyl-β-p-thiogalactopyranoside (IPTG) for 16 hours at 16°C until harvest. Cell pellets were suspended in column buffer (20 mM Tris-HCl, 500 mM NaCl, 1 mM EDTA, and 10% glycerol [pH 8.0]) supplemented with 10 mg/ml of DNase, 1 mM phenylmethylsulfonyl fluoride (PMSF), and $1 \times \text{halt}$ protease inhibitor cocktail (Thermo Fischer Scientific). Three passages through a French pressure cell at 16,000 lb/in² (SLM Aminco, Silver Spring, MD) were performed to lyse the cells before clearing the lysate by centrifugation at $56,000 \times q$ for 1 hour at 4°C. Supernatant fractions were purified through 30 ml of settled chitin-agarose (New England BioLabs) in a column previously equilibrated with column buffer. The intein-CBD tag cleavage was performed using a cleavage buffer (column buffer supplemented with 50 mM dithiothreitol [DTT]) prior to a 48-hour incubation at 4°C. Proteins were eluted with column buffer and concentrated using an Amicon ultrafiltration system with regenerated cellulose membranes (10-kDa cutoff) (Millipore, Billerica, MA) and further purified by fast protein liquid chromatography on a size exclusion HiPrep 26/60 Sephacryl S-200 HR column (GE Healthcare Life Sciences). The column was equilibrated in protein buffer (100 mM Tricine, 150 mM NaCl, 1 mM EDTA, and 15% glycerol [pH 8.0]), and separation was performed at a flow rate of 1 ml/min. Protein-containing fractions were then concentrated by ultrafiltration on regenerated cellulose membranes. Protein concentration was determined using the Bradford protein assay (Bio-Rad).

Differential scanning fluorimetry. Putative McpTPR ligands were investigated by screening phenotype microarray (PM) compounds supplied in a 96-well microplate format (Biolog, Inc., Hayward, CA). For initial high-throughput screening, compounds in PM1, PM2, and PM3B microplates were dissolved in $35\,\mu\text{I}$ of a master mix containing $40\,\mu\text{M}$ McpT^{PR} and $2\times$ Sypro orange (Invitrogen, Grand Island, NY) in the protein buffer. A volume of 30 μ l from each well was transferred to a 96-well plate for use in an ABI 7300 real-time PCR system. Thermal denaturation was carried out by increasing the temperature from 10 to 95°C with a 30-s equilibration at each half degree Celsius. The melting temperature (T_m) of the protein in each well corresponds to the maximum value of the first derivative of the fluorescence curve. The melting temperature shift (ΔT_m) was determined by subtracting the T_m of the control well containing no ligand from the T_m of each test well. The screen was performed in three biological replicates using three Biolog phenotype microarray plates. The compounds that yielded a significant (>2.5°C) positive shift in T., were taken as potential ligands, Initial hits were further tested using known final concentrations (0.4, 4.0, and 40 mM) of each potential ligand to confirm binding. Ligands were prepared in protein buffer, and the experiments were conducted as described above.

Isothermal titration calorimetry. Direct binding studies were performed using a VP-ITC microcalorimeter (Malvern, United Kingdom). All ligand solutions were prepared in the buffer that was eluted from the preparative size exclusion chromatography column. Titrations were all performed at 10 or 20°C, with a stirring speed of 220 rpm, reference power of 25 μ cal/s, and protein in the sample cell. The protein buffer consisted of 0.1 M piperazine-N,N'-bis(2-ethanesulfonic acid) (PIPES) and 0.1 M KCl (pH 7.0). The protein concentration was 45 μ M for the experiments at 10°C and 15 μ M for the experiments at 20°C, except for α -ketobutyrate, citrate, malate, and succinate, which used 45 μ M protein at both temperatures. Ligands were used at the following concentrations for the 10°C experiments: 250 µM oxalate and 2 mM citrate, succinate, malate, malonate, and α -ketobutyrate. Experiments performed at 20°C utilized ligand concentrations of 10 mM citrate and malate, 1 mM malonate, 5 mM succinate and α -ketobutyrate, 2 mM glyoxylate, and 250 μ M oxalate. The titrant was added in 7- to 15- μ l injections at 0.5 μ l/s after an initial 1-µl injection. The final concentration of the titrant was up to 1 mM for the compounds that did not exhibit binding. The dissociation experiment was performed by loading the syringe with $90 \,\mu\text{M}$ McpT^{PR} and making 15- μ l injections of protein in the cell containing only buffer. In dissociation experiments with ligand in buffer solution, the same concentration of ligand was also added to the protein solution. All data were fitted using the VP-ITC version of Origin 7 (Origin Labs, Northampton, MA) and the "one-binding site" model or "dissociation" model where appropriate.

Analytical size exclusion chromatography. Experiments utilized a Superdex 200 increase 10/300 GL column operated by an Äkta pure fast-performance liquid chromatography (FPLC) unit (GE Healthcare, Chicago IL). The injection volume for all samples was 200 μ l, and the column was developed at a flow rate of 0.5 ml/min. A calibration curve was created using 0.1 mg blue dextran (MW of approximately 2,000 kDa), 0.2 mg aldolase (MW, 158 kDa), 0.2 mg conalbumin (MW, 75 kDa), 0.2 mg ovalbumin (MW, 44 kDa), 0.04 mg cytochrome c (MW, 12.4 kDa), and 0.02 mg vitamin B₁₂ (MW, 1.4 kDa). Excluding the native sample, all McpTPR samples were taken from titration experiments and diluted to 30 μ M (corresponding to about 0.11 mg of injected protein). The chromatography buffer was 0.1 M PIPES and 0.1 M KCl (pH 7.0) for the calibration standards and the native protein.

Extraction of seed exudates. Seeds of M. sativa cultivar 'Guardsman II' (100 mg) were rinsed four times with sterile water and then soaked in 3% H₂O₂ for 12 min. The seeds were rinsed four more times with sterile water and placed into an Erlenmeyer flask with 5 ml of sterile water. After an incubation of 24 hours at 30°C, seed exudates were examined under the microscope and plated (20 µl) onto TYC to check for bacterial contamination. Noncontaminated seed exudates were selected, flash frozen in liquid nitrogen, and stored at -80°C.

Quantification of carboxylates in seed exudates by liquid chromatography-mass spectrometry

(LC-MS). Seed exudates from five biological replicates were prepared for analysis by centrifuging for 10 minutes at $10,000 \times g$ before a 1:1 dilution of the sample was prepared with water acidified with 0.1% formic acid. An additional dilution of 1:3 was prepared and analyzed for the quantification of citric and malic acids. The five biological replicates were analyzed with triplicate injections as well as a master mix of all five samples. Quantification of carboxylates in seed exudates was performed on a Shimadzu 9030 high-resolution mass spectrometer (Shimadzu Corp.) interfaced with a Shimadzu 40-B UPLC system (Shimadzu Corp., Kyoto, Japan). The mobile phase was 0.1% formic acid in water held at an isocratic flow at a rate of 0.3 ml/min. Five microliters of sample was injected onto a 150- by 4.6-mm Rezex ROA-organic acid H⁺ column held at 55°C (Phenomenex, Torrance, CA). The mass spectrometer was operated in negative ionization mode with individual carboxylates targeted by selected ion monitoring with a 20-ppm mass window allowance. The mass spectrometer was also programmed to simultaneously collect tandem MS (MS-MS) data for each carboxylate as a secondary confirmation of compound identity. Authentic standards were used to establish compound retention times and calibration curves for quantification. Data were analyzed with Lab Solutions software v5.99 SP2 (Shimadzu Corp.).

SUPPLEMENTAL MATERIAL

Supplemental material is available online only.

SUPPLEMENTAL FILE 1, PDF file, 0.7 MB.

ACKNOWLEDGMENTS

This study was supported by NSF grants MCB-1253234 and MCB-1817652 to B.E.S. The Virginia Tech mass spectrometry incubator is maintained with funding from the Fralin Life Sciences Institute and well as the USDA-NIFA hatch program (VA-160085).

The LC-MS used in this work was provided through a collaboration with Shimadzu Scientific Instruments.

REFERENCES

- Raina J-B, Fernandez V, Lambert B, Stocker R, Seymour JR. 2019. The role of microbial motility and chemotaxis in symbiosis. Nat Rev Microbiol 17:284–294. https://doi.org/10.1038/s41579-019-0182-9.
- Hazelbauer GL, Falke JJ, Parkinson JS. 2008. Bacterial chemoreceptors: highperformance signaling in networked arrays. Trends Biochem Sci 33:9–19. https://doi.org/10.1016/j.tibs.2007.09.014.
- Hoch JA. 2000. Two-component and phosphorelay signal transduction. Curr Opin Microbiol 3:165–170. https://doi.org/10.1016/s1369-5274(00)00070-9.
- Nelson EB. 2004. Microbial dynamics and interactions in the spermosphere. Annu Rev Phytopathol 42:271–309. https://doi.org/10.1146/ annurev.phyto.42.121603.131041.
- Caetano-Anollés G, Wall LG, De Micheli AT, Macchi EM, Bauer WD, Favelukes G. 1988. Role of motility and chemotaxis in efficiency of nodulation by *Rhizobium meliloti*. Plant Physiol 86:1228–1235. https://doi.org/10 .1104/pp.86.4.1228.
- Jones KM, Kobayashi H, Davies BW, Taga ME, Walker GC. 2007. How rhizobial symbionts invade plants: the Sinorhizobium—Medicago model. Nat Rev Microbiol 5:619–633. https://doi.org/10.1038/nrmicro1705.
- Webb BA, Hildreth S, Helm RF, Scharf BE. 2014. Sinorhizobium meliloti chemoreceptor McpU mediates chemotaxis toward host plant exudates through direct proline sensing. Appl Environ Microbiol 80:3404–3415. https://doi.org/10.1128/AEM.00115-14.
- Compton KK, Hildreth SB, Helm RF, Scharf BE. 2018. Sinorhizobium meliloti chemoreceptor McpV senses short-chain carboxylates via direct binding. J Bacteriol 200:e00519-18. https://doi.org/10.1128/JB.00519-18.
- Webb BA, Karl Compton K, Castañeda Saldaña R, Arapov TD, Keith Ray W, Helm RF, Scharf BE. 2017. Sinorhizobium meliloti chemotaxis to quaternary ammonium compounds is mediated by the chemoreceptor McpX. Mol Microbiol 103:333–346. https://doi.org/10.1111/mmi.13561.
- Wall LG, Favelukes G. 1991. Early recognition in the *Rhizobium meliloti*alfalfa symbiosis: root exudate factor stimulates root adsorption of homologous rhizobia. J Bacteriol 173:3492–3499. https://doi.org/10.1128/jb .173.11.3492-3499.1991.
- Mowbray SL, Koshland DE. 1990. Mutations in the aspartate receptor of *Escherichia coli* which affect aspartate binding. J Biol Chem 265:15638– 15643. https://doi.org/10.1016/S0021-9258(18)55445-4.
- Gardina PJ, Bormans AF, Hawkins MA, Meeker JW, Manson MD. 1997. Maltose-binding protein interacts simultaneously and asymmetrically with both

- subunits of the Tar chemoreceptor. Mol Microbiol 23:1181–1191. https://doi.org/10.1046/j.1365-2958.1997.3001661.x.
- 13. Hazelbauer GL. 1975. Maltose chemoreceptor of *Escherichia coli*. J Bacteriol 122:206–214. https://doi.org/10.1128/jb.122.1.206-214.1975.
- 14. Kossmann M, Wolff C, Manson MD. 1988. Maltose chemoreceptor of *Escherichia coli*: interaction of maltose-binding protein and the tar signal transducer. J Bacteriol 170:4516–4521. https://doi.org/10.1128/jb.170.10.4516-4521.1988.
- Hou S, Larsen RW, Boudko D, Riley CW, Karatan E, Zimmer M, Ordal GW, Alam M. 2000. Myoglobin-like aerotaxis transducers in Archaea and Bacteria. Nature 403:540–544. https://doi.org/10.1038/35000570.
- Bibikov SI, Biran R, Rudd KE, Parkinson JS. 1997. A signal transducer for aerotaxis in *Escherichia coli*. J Bacteriol 179:4075–4079. https://doi.org/10 .1128/jb.179.12.4075-4079.1997.
- Falke JJ, Bass RB, Butler SL, Chervitz SA, Danielson MA. 1997. The two-component signaling pathway of bacterial chemotaxis: a molecular view of signal transduction by receptors, kinases, and adaptation enzymes. Annu Rev Cell Dev Biol 13:457–512. https://doi.org/10.1146/annurev.cellbio.13.1.457.
- 18. Wadhams GH, Armitage JP. 2004. Making sense of it all: bacterial chemotaxis. Nat Rev Mol Cell Biol 5:1024–1037. https://doi.org/10.1038/nrm1524.
- Sourjik V, Wingreen NS. 2012. Responding to chemical gradients: bacterial chemotaxis. Curr Opin Cell Biol 24:262–268. https://doi.org/10.1016/j.ceb.2011.11.008.
- Parkinson JS, Hazelbauer GL, Falke JJ. 2015. Signaling and sensory adaptation in *Escherichia coli* chemoreceptors: 2015 update. Trends Microbiol 23:257–266. https://doi.org/10.1016/j.tim.2015.03.003.
- Meier VM, Muschler P, Scharf BE. 2007. Functional analysis of nine putative chemoreceptor proteins in *Sinorhizobium meliloti*. J Bacteriol 189:1816–1826. https://doi.org/10.1128/JB.00883-06.
- Briegel A, Ortega DR, Tocheva El, Wuichet K, Li Z, Chen S, Müller A, Iancu CV, Murphy GE, Dobro MJ, Zhulin IB, Jensen GJ. 2009. Universal architecture of bacterial chemoreceptor arrays. Proc Natl Acad Sci U S A 106:17181–17186. https://doi.org/10.1073/pnas.0905181106.
- Ortega Á, Zhulin IB, Krell T. 2017. Sensory repertoire of bacterial chemoreceptors. Microbiol Mol Biol Rev 81:e00033-17. https://doi.org/10.1128/MMBR .00033-17.
- 24. McKellar JLO, Minnell JJ, Gerth ML. 2015. A high-throughput screen for ligand binding reveals the specificities of three amino acid chemoreceptors from

Pseudomonas syringae pv. actinidiae. Mol Microbiol 96:694-707. https://doi .org/10.1111/mmi.12964.

- 25. Vivoli M, Novak HR, Littlechild JA, Harmer NJ. 2014. Determination of protein-ligand interactions using differential scanning fluorimetry. J Vis Exp e51809. https://doi.org/10.3791/51809.
- 26. Damian L. 2013. Isothermal titration calorimetry for studying protein-ligand interactions, p 103–118. In Williams MA, Daviter T (ed), Protein-ligand interactions: methods and applications. Humana Press, Totowa, NJ.
- 27. Taguchi K, Fukutomi H, Kuroda A, Kato J, Ohtake H. 1997. Genetic identification of chemotactic transducers for amino acids in Pseudomonas aeruginosa. Microbiology 143:3223–3229. https://doi.org/10.1099/00221287-143-10-3223.
- 28. Rico-Jiménez M, Muñoz-Martínez F, García-Fontana C, Fernandez M, Morel B, Ortega Á, Ramos JL, Krell T. 2013. Paralogous chemoreceptors mediate chemotaxis towards protein amino acids and the non-protein amino acid gamma-aminobutyrate (GABA). Mol Microbiol 88:1230-1243. https://doi.org/10.1111/mmi.12255.
- 29. Schäper S, Krol E, Skotnicka D, Kaever V, Hilker R, Søgaard-Andersen L, Becker A. 2016. Cyclic Di-GMP regulates multiple cellular functions in the symbiotic alphaproteobacterium Sinorhizobium meliloti. J Bacteriol 198:521-535. https://doi.org/10.1128/JB.00795-15.
- 30. García V, Reyes-Darias J-A, Martín-Mora D, Morel B, Matilla MA, Krell T. 2015. Identification of a chemoreceptor for C₂ and C₃ carboxylic acids. Appl Environ Microbiol 81:5449-5457. https://doi.org/10.1128/AEM.01529-15.
- 31. Yeh Jl, Biemann H-P, Privé GG, Pandit J, Koshland DE, Jr., Kim S-H. 1996. High-resolution structures of the ligand binding domain of the wild-type bacterial aspartate receptor. J Mol Biol 262:186-201. https://doi.org/10 .1006/jmbi.1996.0507
- 32. Milligan DL, Koshland DE. 1993. Purification and characterization of the periplasmic domain of the aspartate chemoreceptor. J Biol Chem 268:19991-19997. https://doi.org/10.1016/S0021-9258(20)80684-X.
- 33. Rico-Jiménez M, Reyes-Darias JA, Ortega Á, Díez Peña AI, Morel B, Krell T. 2016. Two different mechanisms mediate chemotaxis to inorganic phosphate in Pseudomonas aeruginosa. Sci Rep 6:28967-28967. https://doi .org/10.1038/srep28967.
- 34. Gargallo-Garriga A, Preece C, Sardans J, Oravec M, Urban O, Peñuelas J. 2018. Root exudate metabolomes change under drought and show limited capacity for recovery. Sci Rep 8:12696-12696. https://doi.org/10 .1038/s41598-018-30150-0.
- 35. Gherardi MJ, Rengel Z. 2004. The effect of manganese supply on exudation of carboxylates by roots of lucerne (Medicago sativa). Plant Soil 260:271-282. https://doi.org/10.1023/B:PLSO.0000030182.11473.3b.
- 36. Lopez-Hernandez D, Flores D, Silegert G, Rodrigues JV. 1979. The effect of some orgaic anions on phosphate removal from acid and calcareous soils. Soil Sci 128:312–326. https://doi.org/10.1097/00010694-197912000-00001.
- 37. Earl KD, Syers JK, McLaughlin JR. 1979. Origin of the effects of citrate, tartrate, and acetate on phosphate sorption by soils and synthetic gels. Soil Sci Soc Am J 43:674-678. https://doi.org/10.2136/sssaj1979.03615995004300040009x.
- 38. Tawaraya K, Horie R, Saito S, Wagatsuma T, Saito K, Oikawa A. 2014. Metabolite profiling of root exudates of common bean under phosphorus deficiency. Metabolites 4:599-611. https://doi.org/10.3390/metabo4030599.
- 39. Dunn MF. 1998. Tricarboxylic acid cycle and anaplerotic enzymes in rhizobia. FEMS Microbiol Rev 22:105-123. https://doi.org/10.1111/j.1574-6976 .1998.tb00363.x.
- 40. Iyer B, Rajput MS, Jog R, Joshi E, Bharwad K, Rajkumar S. 2016. Organic acid mediated repression of sugar utilization in rhizobia. Microbiol Res 192:211-220. https://doi.org/10.1016/j.micres.2016.07.006.

- 41. Biondi E, Tatti E, Comparini D, Giuntini E, Mocali S, Giovannetti L, Bazzicalupo M, Mengoni A, Viti C. 2009. Metabolic capacity of Sinorhizobium (Ensifer) meliloti strains as determined byphenotype microArray analysis. Appl Environ Microbiol 75:5396-5404. https://doi.org/10.1128/AEM.00196-09.
- 42. Wheatley RM, Ford BL, Li L, Aroney STN, Knights HE, Ledermann R, East AK, Ramachandran VK, Poole PS. 2020. Lifestyle adaptations of Rhizobium from rhizosphere to symbiosis. Proc Natl Acad Sci U S A 117:23823–23834. https://doi.org/10.1073/pnas.2009094117.
- 43. Zhalnina K, Louie KB, Hao Z, Mansoori N, da Rocha UN, Shi S, Cho H, Karaoz U, Loqué D, Bowen BP, Firestone MK, Northen TR, Brodie EL. 2018. Dynamic root exudate chemistry and microbial substrate preferences drive patterns in rhizosphere microbial community assembly. Nat Microbiol 3:470-480. https://doi.org/10.1038/s41564-018-0129-3.
- 44. Liu X, Zhang K, Liu Y, Xie Z, Zhang C. 2019. Oxalic acid from Sesbania rostrata seed exudates mediates the chemotactic response of Azorhizobium caulinodans ORS571 using multiple strategies. Front Microbiol 10:2727. https://doi.org/10.3389/fmicb.2019.02727.
- 45. Kamberger W. 1979. An Ouchterlony double diffusion study on the interaction between legume lectins and rhizobial cell surface antigens. Arch Microbiol 121:83-90. https://doi.org/10.1007/BF00409209.
- 46. Bertani G. 1951. Studies on lysogenesis I: the mode of phage liberation by lysogenic Escherichia coli. J Bacteriol 62:293–300. https://doi.org/10 .1128/ib.62.3.293-300.1951.
- 47. Scharf B, Schuster-Wolff-Bühring H, Rachel R, Schmitt R. 2001. Mutational analysis of the Rhizobium lupini H13-3 and Sinorhizobium meliloti flagellin genes: importance of flagellin a for flagellar filament structure and transcriptional regulation. J Bacteriol 183:5334-5342. https://doi.org/10.1128/ JB.183.18.5334-5342.2001.
- 48. Götz R, Limmer N, Ober K, Schmitt R. 1982. Motility and chemotaxis in two strains of Rhizobium with complex flagella. Microbiology 128:789-798. https:// doi.org/10.1099/00221287-128-4-789.
- 49. Sourjik V, Schmitt R. 1996. Different roles of CheY1 and CheY2 in the chemotaxis of Rhizobium meliloti. Mol Microbiol 22:427-436. https://doi.org/ 10.1046/j.1365-2958.1996.1291489.x.
- 50. Adler J. 1973. A method for measuring chemotaxis and use of the method to determine optimum conditions for chemotaxis by Escherichia coli. J Gen Microbiol 74:77-91. https://doi.org/10.1099/00221287-74-1-77
- 51. Hanahan D, Meselson M. 1983. Plasmid screening at high colony density. Methods Enzymol 100:333-342. https://doi.org/10.1016/0076-6879(83)00066-x.
- 52. Simon R, O'Connell M, Labes M, Pühler A. 1986. Plasmid vectors for the genetic analysis and manipulation of rhizobia and other gram-negative bacteria. Methods Enzymol 118:640-659. https://doi.org/10.1016/0076 -6879(86)18106-7.
- 53. Pleier E, Schmitt R. 1991. Expression of two Rhizobium meliloti flagellin genes and their contribution to the complex filament structure. J Bacteriol 173:2077-2085. https://doi.org/10.1128/jb.173.6.2077-2085.1991.
- 54. Kovach ME, Elzer PH, Steven Hill D, Robertson GT, Farris MA, Roop RM, Peterson KM. 1995. Four new derivatives of the broad-host-range cloning vector pBBR1MCS, carrying different antibiotic-resistance cassettes. Gene 166:175-176. https://doi.org/10.1016/0378-1119(95)00584-1.
- 55. Bachmann BJ. 1990. Linkage map of Escherichia coli K-12, edition 8. Microbiol Rev 54:130-197. https://doi.org/10.1128/mr.54.2.130-197.1990.
- 56. Novick RP, Clowes RC, Cohen SN, Curtiss R, III, Datta N, Falkow S. 1976. Uniform nomenclature for bacterial plasmids: a proposal. Bacteriol Rev 40:168-189. https://doi.org/10.1128/br.40.1.168-189.1976.